Liquid Crystals
Publication details, including instructions for authors and subscription information:
http://www.informaworld.com/smpp/title~content=t713926090

A new series of chiral nematic bimesogens for the flexoelectro-optic effect

B. Musgrave; P. Lehmann; H. J. Coles

Online publication date: 06 August 2010

To cite this Article Musgrave, B. , Lehmann, P. and Coles, H. J.(1999) 'A new series of chiral nematic bimesogens for the flexoelectro-optic effect', Liquid Crystals, 26: 8, 1235 — 1249
To link to this Article: DOI: 10.1080/026782999204255
URL: http://dx.doi.org/10.1080/026782999204255

LIQUID CRYSTALS, 1999, VOL. 26, NO. 8, 1235–1249

A new series of chiral nematic bimesogens for the flexoelectro-optic effect

B. MUSGRAVE, P. LEHMANN and H. J. COLES*

Department of Physics and Astronomy, Southampton Liquid Crystal Institute, University of Southampton, Highfield, Southampton SO17 1BJ, UK

(*Received 5 February 1999; accepted 25 February 1999*)

A series of chiral bimesogenic compounds has been synthesized. The molecules comprise β-estradiol as the central chiral unit, which is attached to a terminal 4′-cyanobiphenyl-4-yl group at C-17 by an alkanoate spacer containing 5, 6 or 11 carbon atoms. At C-3 the estradiol moiety is substituted with an ω-alkenyloxy chain, also containing 5, 6 or 11 carbon atoms. We will describe the synthesis and phase characterization of these materials. The compounds with 5 or 11 carbon atoms in the spacer separating the mesogens display chiral nematic mesophases with temperature ranges up to 40°C, entering the isotropic state at about 100°C. The pitch lengths of these pure materials are remarkably invariant with temperature. Their electro-optic behaviour has been characterized, with particular emphasis on their flexoelectric properties. The materials have the highest flexoelectric coefficients reported so far in any chiral nematic liquid crystal [with $e(\kappa^{-1}) > +0.5\,\mathrm{C\,N^{-1}\,m^{-1}}$], with flexoelectro-optic response times, for 0 to 90% of transmitted intensity, of the order or less than 1 ms.

1. Introduction

Recently attention has focused on an exceptional electro-optic switching effect originating from the effects of flexoelectricity in short pitch chiral nematic liquid crystals. This flexoelectro-optic switching has a number of advantageous features, being linear with applied electric field [1], being temperature independent [2] and having short response times, often in the microsecond range. Chiral nematic liquid crystals with strong flexoelectric responses have therefore great potential for use in display applications and in optical switches and modulators.

The flexoelectro-optic switching effect was first reported in 1987 [3], and then developed further by the Liquid Crystal Group at Chalmers University, Göteborg [4, 5]. The potential benefits of fast, linear and temperature independent switching at low fields ($\sim$5–10 $\mathrm{V\,\mu m^{-1}}$) have stimulated our interest in the optimization of flexoelectric coefficients by the modification of molecular structure and its subsequent effect on macroscopic performance. At the present time there has been very little experimental work published [4–6] concerning this structure–property relationship.

Dipolar flexoelectric coupling [7] takes place between an electric field and a liquid crystal material when the constituent molecules of the material have a strong electric dipole and an asymmetric shape. In the undeformed state, in zero field, there is no bulk polarization. In the presence of an electric field, however, the asymmetric shape of the molecules causes curvature strains, as the permanent dipoles are forced to align along the field, inducing a macroscopic polarization. Typically, splay deformations are associated with pear-shaped molecules and bend deformations with banana-shaped molecules [7]. In the present work we have synthesized molecules with a shape asymmetry that combines both of these features (i.e. 'pear' and 'banana') with the expectation of combining both splay and bend elastic deformations, shown schematically in figure 1. Since the flexoelectric free energy density contains splay and bend elastic contributions [1, 3, 8] we would then expect the flexoelectro-optic effect to be different, if this hypothesis of shape to deformation correlation is correct. In the present paper we will describe the synthetic route, phase characterization and electro-optic properties of these novel bimesogenic liquid crystals.

2. Theory

An undisturbed chiral nematic is usually described in a Cartesian frame of reference with the z-axis parallel to the helical axis as shown in figure 2(*a*). The director, $\hat{\mathbf{n}}$, is thus confined to the xy-plane with $\hat{\mathbf{n}} = (n_x, n_y, n_z) = (\cos\theta, \sin\theta, 0)$ where θ, taken to be zero when the director is parallel to the x-axis, is given by $\theta = kz$ and $k = 2\pi/P_0$. P_0 is the length of the undisturbed pitch and k is the modulus of the helical wave vector of the material. P_0 is further defined as being positive for a

*Author for correspondence; e-mail: hic@lc.phys.soton.ac.uk

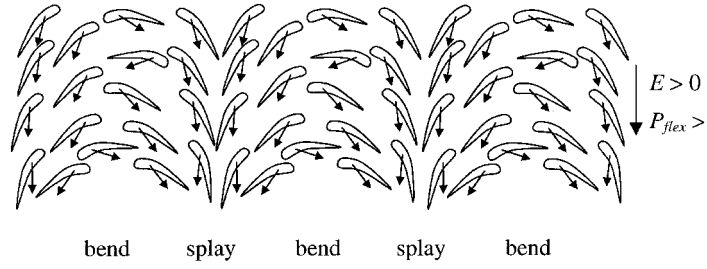

Figure 1. Schematic electric field induced splay–bend deformation patterns in a nematic liquid crystal [8].

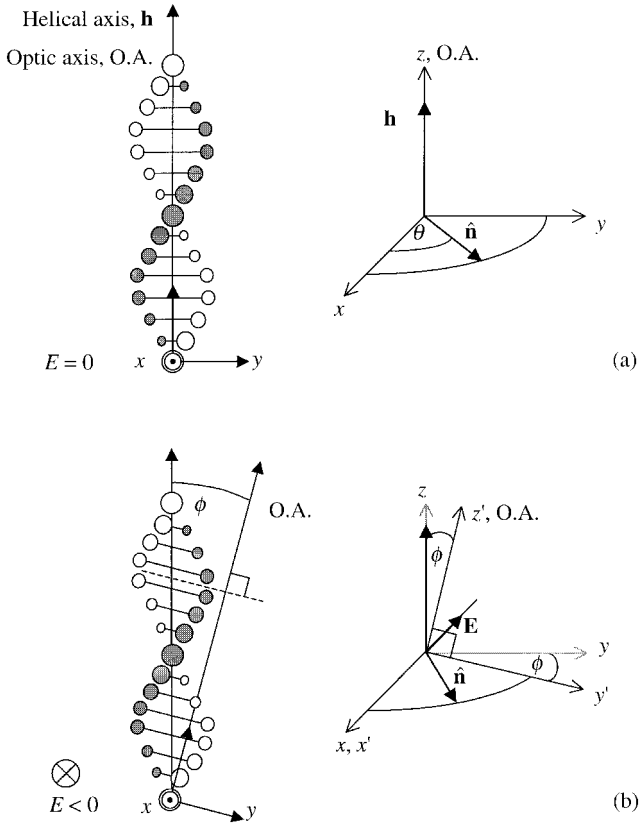

Figure 2. An undisturbed chiral nematic material with a right-handed helix (*a*), with its directors confined to the *xy*-plane, normal to the helical and optic axes. In an electric field applied along the -*x* direction (*b*), the director plane and optic axis are rotated by an angle $+\phi$ about the *x*-axis.

right-handed helix and negative for a left-handed helix. In an undisturbed, short pitch chiral nematic liquid crystal, the optic axis is perpendicular to the mean molecular axis, see figure 2(*a*) [9].

The application of a field along the *x*-axis, a direction perpendicular to the helical axis, causes a rotation of the director plane [3], see figure 2(*b*). In consequence, the optic axis rotates and the transmission properties of the material are altered. The splay and bend deformations due to the flexoelectric coupling form in the rotated director plane. In order to find an expression for this rotation we need to consider the free energy density of the system.

The free energy density, f, of a chiral nematic subject to an electric field may be written in terms of three components, i.e.

$$f = f_{\text{elastic}} + f_{\text{dielectric}} + f_{\text{flexoelectric}} \tag{1}$$

where

$$f_{\text{elastic}} = \frac{1}{2}[\kappa_{11}(\nabla \quad \hat{\mathbf{n}})^2 + \kappa_{22}(k + \hat{\mathbf{n}} \quad \nabla \times \hat{\mathbf{n}})^2 + \kappa_{33}(\hat{\mathbf{n}} \times \nabla \times \hat{\mathbf{n}})^2]$$

and

$$f_{\text{dielectric}} = -\frac{\Delta\varepsilon}{8\pi}(\hat{\mathbf{n}} \quad \mathbf{E})^2 \tag{2}$$

$$f_{\text{flexoelectric}} = -\mathbf{E} \quad (e_s \hat{\mathbf{n}} \nabla \quad \hat{\mathbf{n}} + e_b \hat{\mathbf{n}} \times \nabla \times \hat{\mathbf{n}})$$

where κ_{11}, κ_{22} and κ_{33} are the splay, twist and bend elastic constants of the material, respectively and e_s and e_b are the flexoelectric coefficients of splay and bend, respectively. The dielectric coupling between the dielectric anisotropy, $\Delta\varepsilon = \varepsilon_\parallel - \varepsilon_\perp$ and the field is quadratic in E. The flexoelectric coupling is linear in E and is dominant at low fields for materials with a low $\Delta\varepsilon$. The sign convention for flexoelectric deformations proposed in [8] is used herein.

In the case where $\Delta\varepsilon$ is small but positive, rotation of the optic axis by a small angle ϕ is related to the applied field as follows [3, 10]

$$\tan\phi = \frac{e}{k\kappa}E \tag{3}$$

where e is an effective flexoelectric coefficient [$e = (e_s + e_b)/2$] and κ is an effective elastic constant [$\kappa = (\kappa_{11} + \kappa_{33})/2$]. The angle ϕ is taken as positive when the rotation follows a right-handed screw along the direction of **E** [10].

The coefficient κ varies with the square of the order parameter, S [11]. The dipolar contribution to the coefficient e also varies with temperature as S^2, except where molecules have high conformational freedom, in which case terms that vary linearly with S [12, 13]

may also appear. Where κ and e both vary as S^2, $\tan\phi$ varies as a function of temperature with k^{-1}. Therefore at constant pitch, the tilt angle of the optic axis is temperature-independent.

In the case where the dielectric anisotropy is significant, the dielectric coupling affects the linearity of the response at high fields. Coupling to a material with positive dielectric anisotropy leads to helix-unwinding and, at high fields, to homoeotropic alignment of the director. A large field coupling to a chiral nematic material with negative dielectric anisotropy causes the helix to orient parallel to the applied field.

The characteristic response time, τ, of flexoelectro-optic switching is related to γ_1, the effective viscosity associated with helix distortion (with no liquid flow), and takes the form [14]

$$\tau = \frac{\gamma_1}{\kappa k^2}. \quad (4)$$

Typically, γ_1 ranges in value between 0.01 and 0.1 N s m^{-2} [15]. Thus for a short response time a liquid crystal material with low viscosity and short pitch is required.

Hence, for applications the following properties are essential:

(1) Short pitch, to avoid light diffraction from the helical molecular order, and constant pitch, for a temperature-independent electro-optic response.
(2) Dielectric anisotropy small, to avoid helix unwinding by dielectric coupling, and positive, to allow alignment of the helix perpendicular to the electric field.
(3) Large effective flexoelectric coefficient.
(4) Short response times.

A large flexoelectric coefficient depends on molecular shape and the existence of a strong molecular electric dipole. Via molecular engineering we may hope to synthesize molecules with properties appropriate for the optimization of the flexoelectro-optic effect.

3. Experimental

3.1. *Synthesis*

The bimesogenic liquid crystal materials synthesized for this work contain β-estradiol and 4′-cyanobiphenyl-4-yl units separated by alkyl spacers. The series is denoted *m*Es*n*CB, where Es denotes the chiral estradiol group, CB denotes the highly polar cyanobiphenyl unit and the integers *m* and *n* give the number of carbon atoms in the spacers, as indicated by **7** in the general synthetic route, figure 3.

The commercial reactants were available from Aldrich, Merck and Lancaster. 3,17β-Diydroxyestra-1,3,5(10)-triene was purchased from Sigma. Dichloromethane (DCM) was dried by distillation over P_2O_5. 2-Butanone (MEK) was dried over molecular sieves (4 Å). Silica gel (Silica gel 60, Merck, 0.04–0.063 mm, 230–400 mesh) was used for flash column chromatography.

3.1.1. *17β-Hydroxy-3-(ω-alkenyloxy)estra-1,3,5(10)-triene (**3**)*

A mixture of 20 mmol of 3,17β-Dihydroxyestra-1,3,5(10)-triene (β-Estradiol, **1**), 21 mmol of ω-bromoalk-1-ene (**2**), 21 mmol of Cs_2CO_3 and a catalytic amount of KI in 200 ml of dry MEK was heated under reflux for 2 days under dry N_2. The solvent was evaporated under reduced pressure and DCM was added to the residue. The mixture was filtered and the filtrate concentrated. The crude product was purified by flash column chromatography with DCM/MeOH 200:1 (v/v) as the eluent.

3.1.2. *17β-Hydroxy-3-(4-pentenyloxy)estra-1,3,5(10)-triene (m = 5)*

Yield: 71%. ^{1}H NMR (300 MHz, acetone-d$_6$), δ (ppm): 0.77 (s, 3H, CH_3, C18 (Es)), 1.11–2.19 (m, 16H, CH_2 and CH, C7-8 11-16 (Es), and C2-3 (alkenyloxy)), 2.29 (m, 1H, CH, C9 (Es)), 2.84 (m, 3H, OH, C17 (Es), CH2, C6 (Es)), 3.66 (m, 1H, CH, C17 (Es)), 3.94 (t, $^3J = 6.31$ Hz, 2H, CH_2O), 4.97 (m, $^3J_{cis} = 10.23$ Hz, 1H, H(*E*)H(*Z*)C=), 5.05 (m, $^3J_{trans} = 17.10$ Hz, 1H, H(*E*)H(*Z*)C=), 5.84 (ddt, $^3J_{trans} = 17.10$ Hz, $^3J_{cis} = 10.24$ Hz, $^3J = 6.71$ Hz, 1H, –CH=), 6.62 (d, $^4J = 2.94$ Hz, 1H, ArH, C4 (Es)), 6.68 (dd, $^4J = 2.76$ Hz, $^3J = 8.64$ Hz, 1H, ArH, C2 (Es)), 7.17 (d, $^3J = 8.82$ Hz, 1H, ArH, C1 (Es)). ^{13}C NMR (90 MHz, acetone-d$_6$), δ (ppm): 157.98 (C3 Es), 139.32 (C5 Es), 138.47 (–C=, C4 alkenyloxy) 132.97 (C10 Es), 126.81 (C1 Es), 115.21 (C=, C5 alkenyloxy) 114.82 (C4 Es), 112.55 (C2 Es), 81.59 (C17 Es), 67.93 (C–O, C1 alkenyloxy) 50.71 (C14 Es), 44.70 (C13 Es), 43.82 (C9 Es), 39.75–23.59 (C6,7,8,11,12,15,16 Es, C2,3 alkenyloxy) 11.43 (C18 Es).

3.1.3. *3-(5-Hexenyloxy)-17β-hydroxyestra-1,3,5(10)-triene (m = 6)*

Yield: 75%. ^{1}H NMR (300 MHz, acetone-d$_6$), δ (ppm): 0.76 (s, 3H, CH_3, C18 (Es)), 1.10–2.19 (m, 18H, CH_2 and CH, C7-8 11-16 (Es), and C2-4 (alkenyloxy)), 2.28 (m, 1H, CH, C9 (Es)), 2.84 (m, 3H, OH, C17 (Es), CH2, C6 (Es)), 3.66 (m, 1H, CH, C17 (Es)), 3.93 (t, $^3J = 6.25$ Hz, 2H, CH_2O), 4.95 (m, $^3J_{cis} = 10.29$ Hz, 1H, H(*E*)H(*Z*)C=), 5.03 (m, $^3J_{trans} = 17.10$ Hz, 1H, H(*E*)H(*Z*)C=), 5.84 (ddt, $^3J_{trans} = 17.10$ Hz, $^3J_{cis} = 10.29$ Hz, $^3J = 6.71$ Hz, 1H, –CH=), 6.60 (d, $^4J = 2.94$ Hz, 1H, ArH, C4 (Es)), 6.67 (dd, $^4J = 2.76$ Hz, $^3J = 8.64$ Hz, 1H, ArH, C2 (Es)), 7.16 (d, $^3J = 8.82$ Hz, 1H, ArH, C1 (Es)). ^{13}C NMR (90 MHz, acetone-d$_6$), δ (ppm): 157.70 (C3 Es), 139.33 (C5 Es), 138.25 (–C=, C5 alkenyloxy) 132.97

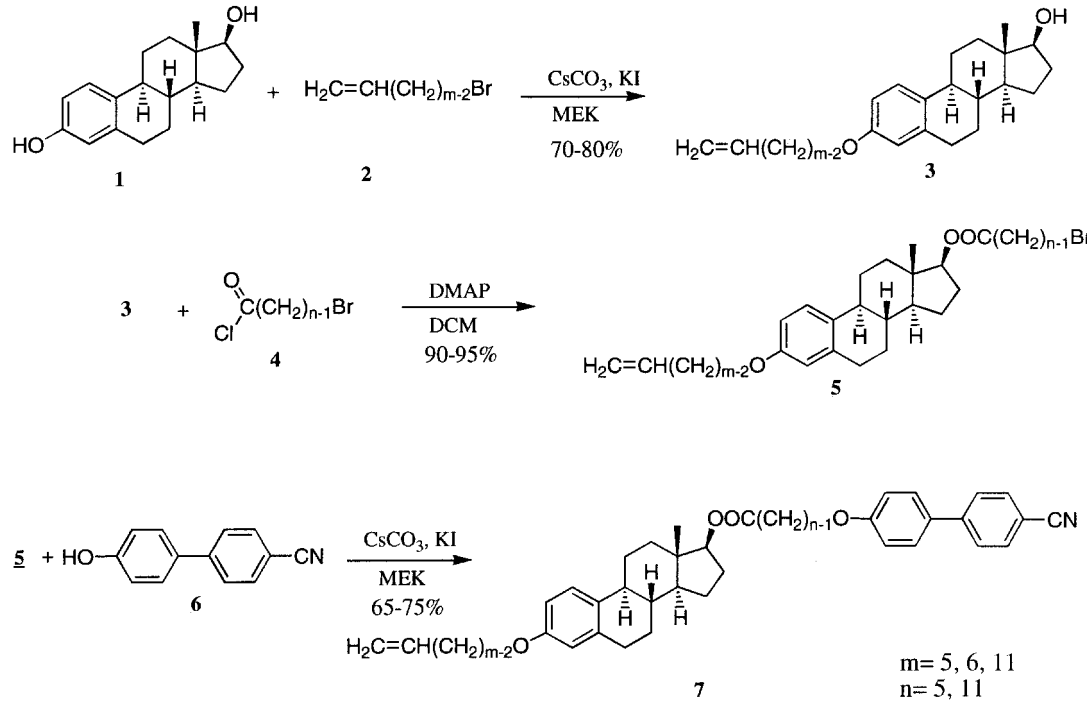

Figure 3. General synthetic route to the bimesogens *m*Es*n*CB.

(C10 Es), 126.81 (C1 Es), 114.88 (C=, C6 alkenyloxy) 114.81 (C4 Es), 112.55 (C2 Es), 81.59 (C17 Es), 67.85 (C–O, C1 alkenyloxy) 50.71 (C14 Es), 44.70 (C13 Es), 43.82 (C9 Es), 39.74–23.59 (C6,7,8,11,12,15,16 Es, C2,3,4 alkenyloxy) 11.43 (C18 Es).

3.1.4. *17β-Hydroxy-3-(10-undecenyloxy)estra-1,3,5(10)-triene (m = 11)*

Yield: 80%. ^{1}H NMR (300 MHz, acetone-d_6), δ (ppm): 0.77 (s, 3H, CH_3, C18 (Es)), 1.10–2.19 (m, 28H, CH_2 and CH, C7-8 11-16 (Es), and C2-9 (alkenyloxy)), 2.28 (m, 1H, CH, C9 (Es)), 2.84 (m, 3H, OH, C17 (Es), CH2, C6 (Es)), 3.66 (m, 1H, CH, C17 (Es)), 3.91 (t, $^3J = 6.43$ Hz, 2H, CH_2O), 4.92 (m, $^3J_{cis} = 10.15$ Hz, 1H, H(*E*)H(*Z*)C=), 4.99 (m, $^3J_{trans} = 17.19$ Hz, 1H, H(*E*)H(*Z*)C=), 5.81 (ddt, $^3J_{trans} = 17.04$ Hz, $^3J_{cis} = 10.23$ Hz, $^3J = 6.71$ Hz, 1H, –CH=), 6.59 (d, $^4J = 2.94$ Hz, 1H, ArH, C4 (Es)), 6.66 (dd, $^4J = 2.76$ Hz, $^3J = 8.64$ Hz, 1H, ArH, C2 (Es)), 7.15 (d, $^3J = 8.82$ Hz, 1H, ArH, C1 (Es)). ^{13}C NMR (90 MHz, acetone-d_6), δ (ppm): 157.69 (C3 Es), 139.34 (C5 Es), 139.23 (–C=, C10 alkenyloxy) 132.95 (C10 Es), 126.81 (C1 Es), 114.81 (C=, C11 alkenyloxy) 114.82 (C4 Es), 112.53 (C2 Es), 81.58 (C17 Es), 67.85 (C–O, C1 alkenyloxy) 50.70 (C14 Es), 44.71 (C13 Es), 43.83 (C9 Es), 39.74–23.58 (C6,7,8,11,12,15,16 Es, C2,3,4 alkenyloxy) 11.42 (C18 Es).

3.1.5. *ω-Bromoalkanoyl chloride (**4**)*

Oxalyl chloride (5 eq.) was added slowly to a suspension (solution), of the appropriate ω-bromoalkanoic acid in benzene at 0°C under dry N_2. The reaction mixture was allowed to warm to room temperature overnight. The solvent and excess of oxalyl chloride were distilled off and the residue was dried for one day under high vacuum. The acid chlorides were used without further purification.

3.1.6. *3-(ω-Alkenyloxy)estra-1,3,5(10)-triene-17β-yl ω-Bromoalkanoate (**5**)*

The appropriate ω-bromoalkanoyl chloride **4** (6 mmol) in 10 ml of dry DCM were added dropwise to a solution of 5 mmol of **3** and 6.3 mmol of DMAP in 25 ml of dry DCM at 0°C under dry N_2. The reaction mixture was allowed to warm to room temperature overnight. DCM was added and the solution was washed three times with 1M HCl, dried over $MgSO_4$ and concentrated. The crude product was purified by flash column chromatography with DCM/PE 2:1 (v/v) as the eluent.

3.1.7. *3-(4-Pentenyloxy)estra-1,3,5(10)-triene-17β-yl 5-bromopentanoate (m = 5, n = 5)*

Yield: 90%. ^{1}H NMR (300 MHz, $CDCl_3$) δ (ppm): 0.84 (s, 3H, CH_3, C18 (Es)), 1.14–2.40 (m, 23H, CH_2 and CH, C7-16 (Es), C2-3 (alkenyloxy) and C2-4 (alkanoate)), 2.84 (m, 2H, CH_2, C6 (Es)), 3.44 (t, $^3J = 6.62$ Hz, 2H, CH_2Br), 3.95 (t, $^3J = 6.43$ Hz, 2H, CH_2O), 4.71 (dd, $^3J = 9.00$ Hz, $^3J = 7.54$ Hz, 1H, CH, C17 (Es)), 5.00 (m, $^3J_{cis} = 10.22$ Hz, 1H, H(*E*)H(*Z*)C=), 5.07 (m, $^3J_{trans} = 17.10$ Hz, 1H, H(*E*)H(*Z*)C=), 5.86 (ddt, $^3J_{trans} = 17.04$ Hz, $^3J_{cis} = 10.11$ Hz, $^3J = 6.71$ Hz, 1H,

–CH=), 6.64 (d, $^4J = 2.57$ Hz, 1H, ArH, C4 (Es)), 6.71 (dd, $^4J = 2.94$ Hz, $^3J = 8.46$ Hz, 1H, ArH, C2 (Es)), 7.20 (d, $^3J = 8.46$ Hz, 1H, ArH, C1 (Es)). ^{13}C NMR (90 MHz, $CDCl_3$) δ (ppm): 173.60 (COO), 157.09 (C3 Es), 138.69 (C5 Es), 138.01 (–C=, C4 alkenyloxy) 132.74 (C10 Es), 126.45 (C1 Es), 115.22 (C=, C5 alkenyloxy) 114.63 (C4 Es), 112.18 (C2 Es), 82.70 (C17 Es), 67.70 (C–O, C1 alkenyloxy) 49.84 (C14 Es), 43.88 (C13 Es), 43.08 (C9 Es), 38.69–23.37 (C6,7,8,11,12,15,16 Es, C2-3 alkenyloxy, C2-5 alkanoate), 12.23 (C18 Es).

3.1.8. *3-(5-Hexenyloxy)estra-1,3,5(10)-triene-17β-yl 5-bromopentanoate (m = 6, n = 5)*

Yield: 92%. ^{1}H NMR (300 MHz, $CDCl_3$) δ (ppm): 0.84 (s, 3H, CH_3, C18 (Es)), 1.14–2.40 (m, 25H, CH_2 and CH, C7-16 (Es), C2-4 (alkenyloxy) and C2-4 (alkanoate)), 2.84 (m, 2H, CH_2, C6 (Es)), 3.44 (t, $^3J = 6.62$ Hz, 2H, CH_2Br), 3.95 (t, $^3J = 6.43$ Hz, 2H, CH_2O), 4.71 (dd, $^3J = 9.00$ Hz, $^3J = 7.54$ Hz, 1H, CH, C17 (Es)), 5.00 (m, $^3J_{cis} = 10.22$ Hz, 1H, H(*E*)H(*Z*)C=), 5.07 (m, $^3J_{trans} = 17.10$ Hz, 1H, H(*E*)H(*Z*)C=), 5.86 (ddt, $^3J_{trans} = 17.04$ Hz, $^3J_{cis} = 10.11$ Hz, $^3J = 6.71$ Hz, 1H, –CH=), 6.64 (d, $^4J = 2.57$ Hz, 1H, ArH, C4 (Es)), 6.71 (dd, $^4J = 2.94$ Hz, $^3J = 8.46$ Hz, 1H, ArH, C2 (Es)), 7.20 (d, $^3J = 8.46$ Hz, 1H, ArH, C1 (Es)). ^{13}C NMR (90 MHz, $CDCl_3$) δ (ppm): 173.61 (COO), 157.06 (C3 Es), 138.69 (C5 Es), 137.91 (–C=, C5 alkenyloxy) 132.39 (C10 Es), 126.39 (C1 Es), 114.78 (C=, C6 alkenyloxy) 114.52 (C4 Es), 112.07 (C2 Es), 82.69 (C17 Es), 67.71 (C–O, C1 alkenyloxy) 49.85 (C14 Es), 43.86 (C13 Es), 43.06 (C9 Es), 38.67–23.35 (C6,7,8,11,12,15,16 Es, C2-4 alkenyloxy, C2-5 alkanoate), 12.25 (C18 Es).

3.1.9. *3-(10-Undecenyloxy)estra-1,3,5(10)-triene-17β-yl 5-bromopentanoate (m = 11, n = 5)*

Yield: 90%. ^{1}H NMR (300 MHz, $CDCl_3$) δ (ppm): 0.84 (s, 3H, CH_3, C18 (Es)), 1.14–2.49 (m, 35H, CH_2 and CH, C7-16 (Es), C2-9 (alkenyloxy) and C2-4 (alkanoate)), 2.84 (m, 2H, CH_2, C6 (Es)), 3.44 (t, $^3J = 6.62$ Hz, 2H, CH_2Br), 3.93 (t, $^3J = 6.43$ Hz, 2H, CH_2O), 4.71 (dd, $^3J = 9.00$ Hz, $^3J = 7.54$ Hz, 1H, CH, C17 (Es)), 4.94 (m, $^3J_{cis} = 10.37$ Hz, 1H, H(*E*)H(*Z*)C=), 5.01 (m, $^3J_{trans} = 17.10$ Hz, 1H, H(*E*)H(*Z*)C=), 5.83 (ddt, $^3J_{trans} = 17.04$ Hz, $^3J_{cis} = 10.17$ Hz, $^3J = 6.66$ Hz, 1H, –CH=), 6.64 (d, $^4J = 2.57$ Hz, 1H, ArH, C4 (Es)), 6.71 (dd, $^4J = 2.76$ Hz, $^3J = 8.64$ Hz, 1H, ArH, C2 (Es)), 7.19 (d, $^3J = 8.46$ Hz, 1H, ArH, C1 (Es)). ^{13}C NMR (90 MHz, $CDCl_3$) δ (ppm): 173.34 (COO), 157.17 (C3 Es), 139.39 (C5 Es), 137.98 (–C=, C10 alkenyloxy) 132.39 (C10 Es), 126.44 (C1 Es), 114.60 (C=, C11 alkenyloxy) 114.28 (C4 Es), 112.17 (C2 Es), 82.91 (C17 Es), 68.03 (C–O, C1 alkenyloxy) 49.90 (C14 Es), 43.94 (C13 Es), 43.13 (C9 Es), 38.73–23.43 (C6,7,8,11,12,15,16 Es, C2-9 alkenyloxy, C2-5 alkanoate), 12.22 (C18 Es).

3.1.10. *3-(4-Pentenyloxy)estra-1,3,5(10)-triene-17β-yl 6-bromohexanoate (m = 5, n = 6)*

Yield: 93%. ^{1}H NMR (300 MHz, $CDCl_3$) δ (ppm): 0.84 (s, 3H, CH_3, C18 (Es)), 1.14–2.40 (m, 25H, CH_2 and CH, C7-16 (Es), C2-3 (alkenyloxy) and C2-5 (alkanoate)), 2.84 (m, 2H, CH_2, C6 (Es)), 3.44 (t, $^3J = 6.62$ Hz, 2H, CH_2Br), 3.95 (t, $^3J = 6.43$ Hz, 2H, CH_2O), 4.71 (dd, $^3J = 9.00$ Hz, $^3J = 7.54$ Hz, 1H, CH, C17 (Es)), 5.00 (m, $^3J_{cis} = 10.22$ Hz, 1H, H(*E*)H(*Z*)C=), 5.07 (m, $^3J_{trans} = 17.10$ Hz, 1H, H(*E*)H(*Z*)C=), 5.86 (ddt, $^3J_{trans} = 17.04$ Hz, $^3J_{cis} = 10.11$ Hz, $^3J = 6.71$ Hz, 1H, –CH=), 6.64 (d, $^4J = 2.57$ Hz, 1H, ArH, C4 (Es)), 6.71 (dd, $^4J = 2.94$ Hz, $^3J = 8.46$ Hz, 1H, ArH, C2 (Es)), 7.20 (d, $^3J = 8.46$ Hz, 1H, ArH, C1 (Es)), ^{13}C NMR (90 MHz, $CDCl_3$) δ (ppm): 173.61 (COO), 157.09 (C3 Es), 138.69 (C5 Es), 138.01 (–C=, C4 alkenyloxy) 132.74 (C10 Es), 126.45 (C1 Es), 115.22 (C=, C5 alkenyloxy) 114.63 (C4 Es), 112.18 (C2 Es), 82.69 (C17 Es), 67.71 (C–O, C1 alkenyloxy) 49.85 (C14 Es), 43.86 (C13 Es), 43.06 (C9 Es), 38.67–23.35 (C6,7,8,11,12,15,16 Es, C2-3 alkenyloxy, C2-6 alkanoate), 12.24 (C18 Es).

3.1.11. *3-(5-Hexenyloxy)estra-1,3,5(10)-triene-17β-yl 6-bromohexanoate (m = 6, n = 6)*

Yield: 94%. ^{1}H NMR (300 MHz, $CDCl_3$) δ (ppm): 0.84 (s, 3H, CH_3, C18 (Es)), 1.14–2.40 (m, 27H, CH_2 and CH, C7-16 (Es), C2-4 (alkenyloxy) and C2-5 (alkanoate)), 2.84 (m, 2H, CH_2, C6 (Es)), 3.44 (t, $^3J = 6.62$ Hz, 2H, CH_2Br), 3.95 (t, $^3J = 6.43$ Hz, 2H, CH_2O), 4.71 (dd, $^3J = 9.00$ Hz, $^3J = 7.54$ Hz, 1H, CH, C17 (Es)), 5.00 (m, $^3J_{cis} = 10.22$ Hz, 1H, H(*E*)H(*Z*)C=), 5.07 (m, $^3J_{trans} = 17.10$ Hz, 1H, H(*E*)H(*Z*)C=), 5.86 (ddt, $^3J_{trans} = 17.04$ Hz, $^3J_{cis} = 10.11$ Hz, $^3J = 6.71$ Hz, 1H, –CH=), 6.64 (d, $^4J = 2.57$ Hz, 1H, ArH, C4 (Es)), 6.71 (dd, $^4J = 2.94$ Hz, $^3J = 8.46$ Hz, 1H, ArH, C2 (Es)), 7.20 (d, $^3J = 8.46$ Hz, 1H, ArH, C1 (Es)). ^{13}C NMR (90 MHz, $CDCl_3$) δ (ppm): 173.59 (COO), 157.05 (C3 Es), 138.69 (C5 Es), 137.91 (–C=, C5 alkenyloxy) 132.39 (C10 Es), 126.38 (C1 Es), 114.77 (C=, C6 alkenyloxy) 114.51 (C4 Es), 112.08 (C2 Es), 82.70 (C17 Es), 67.70 (C–O, C1 alkenyloxy) 49.84 (C14 Es), 43.87 (C13 Es), 43.06 (C9 Es), 38.67–23.36 (C6,7,8,11,12,15,16 Es, C2-4 alkenyloxy, C2-6 alkanoate), 12.23 (C18 Es).

3.1.12. *3-(4-Pentenyloxy)estra-1,3,5(10)-triene-17β-yl 11-bromoundecanoate (m = 5, n = 11)*

Yield: 95%. ^{1}H NMR (300 MHz, $CDCl_3$) δ (ppm): 0.84 (s, 3H, CH_3, C18 (Es)), 1.14–2.40 (m, 35H, CH_2 and CH, C7-16 (Es), C2-3 (alkenyloxy) and C2-10 (alkanoate)), 2.84 (m, 2H, CH_2, C6 (Es)), 3.42 (t, $^3J = 6.80$ Hz, 2H, CH_2Br), 3.95 (t, $^3J = 6.43$ Hz, 2H, CH_2O), 4.71 (dd, $^3J = 9.00$ Hz, $^3J = 7.54$ Hz, 1H, CH, C17 (Es)), 5.00 (m, $^3J_{cis} = 10.22$ Hz, 1H, H(*E*)H(*Z*)C=), 5.07 (m, $^3J_{trans} = 17.10$ Hz, 1H, H(*E*)H(*Z*)C=), 5.86

(ddt, $^3J_{trans} = 17.04$ Hz, $^3J_{cis} = 10.11$ Hz, $^3J = 6.71$ Hz, 1H, –CH=), 6.64 (d, $^4J = 2.57$ Hz, 1H, ArH, C4 (Es)), 6.71 (dd, $^4J = 2.94$ Hz, $^3J = 8.46$ Hz, 1H, ArH, C2 (Es)), 7.20 (d, $^3J = 8.46$ Hz, 1H, ArH, C1 (Es)). ^{13}C NMR (90 MHz, $CDCl_3$) δ (ppm): 174.12 (COO), 157.07 (C3 Es), 138.08 (C5 Es), 138.01 (–C=, C4 alkenyloxy) 132.55 (C10 Es), 126.46 (C1 Es), 115.26 (C=, C5 alkenyloxy) 114.62 (C4 Es), 112.17 (C2 Es), 82.60 (C17 Es), 67.21 (C–O, C1 alkenyloxy) 49.93 (C14 Es), 43.96 (C13 Es), 43.12 (C9 Es), 38.74–23.44 (C6,7,8,11,12,15,16 Es, C2,3 alkenyloxy, C2-11 alkanoate), 12.27 (C18 Es).

3.1.13. *3-(10-Undecenyloxy)estra-1,3,5(10)-triene-17β-yl 11-bromoundecanoate (m = 11, n = 11)*

Yield: 95%. ^{1}H NMR (300 MHz, $CDCl_3$) δ (ppm): 0.84 (s, 3H, CH_3, C18 (Es)), 1.14–2.40 (m, 47H, CH_2 and CH, C7-16 (Es), C2-9 (alkenyloxy) and C2-10 (alkanoate)), 2.84 (m, 2H, CH_2, C6 (Es)), 3.42 (t, $^3J = 6.80$ Hz, 2H, CH_2 Br), 3.93 (t, $^3J = 6.43$ Hz, 2H, CH_2 O), 4.71 (dd, $^3J = 9.00$ Hz, $^3J = 7.54$ Hz, 1H, CH, C17 (Es)), 4.94 (m, $^3J_{cis} = 10.37$ Hz, 1H, H(*E*)H(*Z*)C=), 5.01 (m, $^3J_{trans} = 17.10$ Hz, 1H, H(*E*)H(*Z*)C=), 5.83 (ddt, $^3J_{trans} = 17.10$ Hz, $^3J_{cis} = 10.17$ Hz, $^3J = 6.66$ Hz, 1H, –CH=), 6.64 (d, $^4J = 2.57$ Hz, 1H, ArH, C4 (Es)), 6.71 (dd, $^4J = 2.76$ Hz, $^3J = 8.46$ Hz, 1H, ArH, C2 (Es)), 7.19 (d, $^3J = 8.47$ Hz, 1H, ArH, C1 (Es)). ^{13}C NMR (90 MHz, $CDCl_3$) δ (ppm): 174.12 (COO), 157.17 (C3 Es), 139.39 (C5 Es), 137.97 (–C=, C10 alkenyloxy) 132.39 (C10 Es), 126.44 (C1 Es), 114.60 (C=, C11 alkenyloxy) 114.28 (C4 Es), 112.17 (C2 Es), 82.61 (C17 Es), 68.03 (C–O, C1 alkenyloxy) 49.92 (C14 Es), 43.96 (C13 Es), 43.13 (C9 Es), 38.74–23.44 (C6,7,8,11,12,15,16 Es, C2,9 alkenyloxy, C2-11 alkanoate), 12.27 (C18 Es).

3.1.14. *3-(ω-Alkenyloxy)estra-1,3,5(10)-triene-17β-yl ω-(4′-cyanobiphenyl-4-yloxy)alkanoate (**7**)*

A mixture of 4 mmol of **5**, 4.8 mmol of 4-cyano-4′-hydroxybiphenyl (**6**), 5 mmol of Cs_2CO_3 and a catalytic amount of KI in 50 ml of dry MEK was heated under reflux for 1 day under dry N_2. The solvent was evaporated under reduced pressure and DCM was added to the residue. The mixture was filtered and the filtrate concentrated. The crude product was purified by flash column chromatography with DCM as the eluent.

3.1.15. *3-(4-Pentenyloxy)estra-1,3,5(10)-triene-17β-yl 5-(4′-cyanobiphenyl-4-yloxy)pentanoate (5Es5CB)*

Yield: 73%, $C_{41}H_{47}NO_4$, Ms(ESI): *m/z*: 635.7 (100% $(M + NH_4)^+$, calc.: 635.4), 618.7 (35% $(M + H)^+$, calc.: 618.8). ^{1}H NMR (300 MHz, $CDCl_3$) δ (ppm): 0.84 (s, 3H, CH_3, C18 (Es)), 1.15–2.49 (m, 23H, CH_2 and CH, C7-16 (Es), C2-3 (alkenyloxy) and C2-4 (alkanoate)), 2.84 (m, 2H, CH_2, C6 (Es)), 3.95 (t, $^3J = 6.43$ Hz, 2H, $CH_2OAr_{(Es)}$), 4.02 (t, $^3J = 6.43$ Hz, 2H, $CH_2OAr_{(CB)}$), 5.00 (m, $^3J_{cis} = 10.22$ Hz, 1H, H(*E*)H(*Z*)C=), 5.07 (m, $^3J_{trans} = 17.10$ Hz, 1H, H(*E*)H(*Z*)C=), 5.86 (ddt, $^3J_{trans} = 17.04$ Hz, $^3J_{cis} = 10.11$ Hz, $^3J = 6.71$ Hz, 1H, –CH=), 6.63 (d, $^4J = 2.57$ Hz, 1H, ArH, C4 (Es)), 6.70 (dd, $^4J = 2.57$ Hz, $^3J = 8.46$ Hz, 1H, ArH, C2 (Es)), 7.00 (m, $^3J = 6.62$ Hz, 2H, ArH, C3+5 (CB)), 7.20 (d, $^3J = 8.46$ Hz, 1H, ArH, C1 (Es)), 7.54 (m, $^3J = 6.62$ Hz, 2H, ArH, C2+6 (CB)), 7.65 (m, $^3J = 6.62$ Hz, 2H, ArH, C2′+6′ (CB)), 7.70 (m, $^3J = 6.62$ Hz, 2H, ArH, C3′+5′ (CB)). ^{13}C NMR (90 MHz, $CDCl_3$) δ (ppm): 173.60 (COO), 159.76 (C4 CB), 157.09 (C3 Es), 145.38 (C1′ CB), 138.09 (C5 Es), 138.01 (–C=, C4 alkenyloxy) 132.72 (C3′,5′ CB), 132.49 (C10 Es), 131.56 (C1 CB), 128.51 (C2,6 CB), 127.23 (C2′,6′ CB), 126.45 (C1 Es), 119.29 (CN), 115.27 (C3,5 CB), 115.22 (C=, C5 alkenyloxy) 114.63 (C4 Es), 112.17 (C2 Es), 110.22 (C4′ CB), 82.84 (C17 Es), 67.70 (C–O, C5 alkanoate), 67.213 (C–O, C1 alkenyloxy) 49.92 (C14 Es), 43.95 (C13 Es), 43.15 (C9 Es), 38.73–21.93 (C6,7,8,11,12,15,16 Es, C2-3 alkenyloxy, C2-4 alkanoate), 12.32 (C18 Es).

3.1.16. *3-(5-Hexenyloxy)estra-1,3,5(10)-triene-17β-yl 5-(4′-cyanobiphenyl-4-yloxy)pentanoate (6Es5CB)*

Yield: 68%, $C_{42}H_{49}NO_4$ Ms(ESI): *m/z*: 649.4 (100% $(M + NH_4)^+$, calc.: 649.4), 618.7 (25% $(M + H)^+$, calc.: 632.6). ^{1}H NMR (300 MHz, $CDCl_3$) δ (ppm): 0.84 (s, 3H, CH_3, C18 (estradiol)), 1.15–2.49 (m, 25H, CH_2 and CH, C7-16 (Es), C2-4 (alkenyloxy) and C2-4 (alkanoate)), 2.84 (m, 2H, CH_2, C6 (Es)), 3.95 (t, $^3J = 6.43$ Hz, 2H, $CH_2OAr_{(Es)}$), 4.02 (t, $^3J = 6.43$ Hz, 2H, $CH_2OAr_{(CB)}$), 5.00 (m, $^3J_{cis} = 10.22$ Hz, 1H, H(*E*)H(*Z*)C=), 5.07 (m, $^3J_{trans} = 17.10$ Hz, 1H, H(*E*)H(*Z*)C=), 5.86 (ddt, $^3J_{trans} = 17.04$ Hz, $^3J_{cis} = 10.11$ Hz, $^3J = 6.71$ Hz, 1H, –CH=), 6.63 (d, $^4J = 2.57$ Hz, 1H, ArH, C4 (Es)), 6.70 (dd, $^4J = 2.57$ Hz, $^3J = 8.46$ Hz, 1H, ArH, C2 (Es)), 7.00 (m, $^3J = 6.62$ Hz, 2H, ArH, C3+5 (CB)), 7.20 (d, $^3J = 8.46$ Hz, 1H, ArH, C1 (Es)), 7.54 (m, $^3J = 6.62$ Hz, 2H, ArH, C2+6 (CB)), 7.65 (m, $^3J = 6.62$ Hz, 2H, ArH, C2′+6′ (CB)), 7.70 (m, $^3J = 6.62$ Hz, 2H, ArH, C3′+5′ (CB)). ^{13}C NMR (90 MHz, $CDCl_3$) δ (ppm): 173.58 (COO), 159.74 (C4 CB), 157.11 (C3 Es), 145.40 (C1′ CB), 138.08 (C5 Es), 137.99 (–C=, C5 alkenyloxy) 132.71 (C3′,5′ CB), 132.47 (C10 Es), 131.58 (C1 CB), 128.50 (C2,6 CB), 127.23 (C2′,6′ CB), 126.43 (C1 Es), 119.31 (CN), 115.27 (C3,5 CB), 115.15 (C=, C6 alkenyloxy) 114.62 (C4 Es), 112.17 (C2 Es), 110.19 (C4′ CB), 82.81 (C17 Es), 67.68 (C–O,C5 alkanoate), 67.19 (C–O,C1 alkenyloxy) 49.94 (C14 Es), 43.95 (C13 Es), 43.14 (C9 Es), 38.73–21.92 (C6,7,8,11,12,15,16 Es, C2-4 alkenyloxy, C2-4 alkanoate), 12.32 (C18 Es).

3.1.17. *3-(10-Undecenyloxy)estra-1,3,5(10)-triene-17β-yl 5-(4′-cyanobiphenyl-4-yloxy)pentanoate (11Es5CB)*

Yield: 65%, $C_{47}H_{59}NO_4$ Ms(ESI): *m/z*: 719.6 (100% $(M + NH_4)^+$, calc.: 719.5), 702.6 (23% $(M + H)^+$,

calc.: 702.4). ^{1}H NMR (300 MHz, $CDCl_3$) δ (ppm): 0.84 (s, 3H, CH_3, C18 (Es)), 1.15–2.49 (m, 35H, CH_2 and CH, C7-16 (Es), C2-9 (alkenyloxy) and C2-4 (alkanoate)), 2.84 (m, 2H, CH_2, C6 (Es)), 3.92 (t, $^3J = 6.43$ Hz, 2H, $CH_2OAr_{(Es)}$), 4.02 (t, $^3J = 6.43$ Hz, 2H, $CH_2OAr_{(CB)}$), 4.71 (dd, $^3J = 9.00$ Hz, $^3J = 7.54$ Hz, 1H, CH, C17 (Es)), 4.94 (m, $^3J_{cis} = 10.37$ Hz, 1H, H(*E*)H(*Z*)C=), 5.01 (m, $^3J_{trans} = 17.10$ Hz, 1H, H(*E*)H(*Z*)C=), 5.83 (ddt, $^3J_{trans} = 17.04$ Hz, $^3J_{cis} = 10.17$ Hz, $^3J = 6.66$ Hz, 1H, –CH=), 6.63 (d, $^4J = 2.57$ Hz, 1H, ArH, C4 (Es)), 6.70 (dd, $^4J = 2.57$ Hz, $^3J = 8.46$ Hz, 1H, ArH, C2 (Es)), 7.00 (m, $^3J = 6.62$ Hz, 2H, ArH, C3+5 (CB)), 7.19 (d, $^3J = 8.46$ Hz, 1H, ArH, C1 (Es)), 7.54 (m, $^3J = 6.62$ Hz, 2H, ArH, C2+6 (CB)), 7.65 (m, $^3J = 6.62$ Hz, 2H, ArH, C2′+6′ (CB)), 7.70 (m, $^3J = 6.62$ Hz, 2H, ArH, C3′+5′ (CB)). ^{13}C NMR (90 MHz, $CDCl_3$) δ (ppm): 174.13 (COO), 159.95 (C4 CB), 157.17 (C3 Es), 145.44 (C1′ CB), 139.40 (C5 Es), 137.98 (–C=, C10 alkenyloxy) 132.72 (C3′,5′ CB), 132.42 (C10 Es), 131.39 (C1 CB), 128.47 (C2,6 CB), 127.23 (C2′,6′ CB), 126.43 (C1 Es), 119.29 (CN), 115.23 (C3,5 CB), 114.60 (C=, C11 alkenyloxy) 114.28 (C4 Es), 112.17 (C2 Es), 110.17 (C4′ CB), 82.61 (C17 Es), 68.31 (C–O, C5 alkanoate), 68.03 (C–O, C1 alkenyloxy) 49.92 (C14 Es), 68.31 (C–O, C5 alkanoate), 68.03 (C–O, C1 alkenyloxy) 49.92 (C14 Es), 43.95 (C13 Es), 43.13 (C9 Es), 38.75–23.44 (C6,7,8,11,12,15,16 Es, C2-9 alkenyloxy, C2-4 alkanoate), 12.28 (C18 Es).

3.1.18. *3-(4-Pentenyloxy)estra-1,3,5(10)-triene-17β-yl 6-(4′-cyanobiphenyl-4-yloxy)hexanoate (5Es6CB)*

Yield: 69%, $C_{42}H_{49}NO_4$ Ms(ESI): *m/z*: 649.8 (100%$(M+NH_4)^+$, calc.: 649.4), 632.8 (22%$(M+H)^+$, calc.: 632.4). ^{1}H NMR (300 MHz, $CDCl_3$) δ (ppm): 0.84 (s, 3H, CH_3, C18 (Es)), 1.15–2.49 (m, 25H, CH_2 and CH, C7-16 (Es), C2-3 (alkenyloxy) and C2-5 (alkanoate)), 2.84 (m, 2H, CH_2, C6 (Es)), 3.95 (t, $^3J = 6.43$ Hz, 2H, $CH_2OAr_{(Es)}$), 4.02 (t, $^3J = 6.43$ Hz, 2H, $CH_2OAr_{(CB)}$), 5.00 (m, $^3J_{cis} = 10.22$ Hz, 1H, H(*E*)H(*Z*)C=), 5.07 (m, $^3J_{trans} = 17.10$ Hz, 1H, H(*E*)H(*Z*)C=), 5.86 (ddt, $^3J_{trans} = 17.04$ Hz, $^3J_{cis} = 10.11$ Hz, $^3J = 6.71$ Hz, 1H, –CH=), 6.63 (d, $^4J = 2.57$ Hz, 1H, ArH, C4 (Es)), 6.70 (dd, $^4J = 2.57$ Hz, $^3J = 8.46$ Hz, 1H, ArH, C2 (Es)), 7.00 (m, $^3J = 6.62$ Hz, 2H, ArH, C3+5 (CB)), 7.20 (d, $^3J = 8.46$ Hz, 1H, ArH, C1 (Es)), 7.54 (m, $^3J = 6.62$ Hz, 2H, ArH, C2+6 (CB)), 7.65 (m, $^3J = 6.62$ Hz, 2H, ArH, C2′+6′ (CB)), 7.70 (m, $^3J = 6.62$ Hz, 2H, ArH, C3′+5′ (CB)). ^{13}C NMR (90 MHz, $CDCl_3$) δ (ppm): 173.60 (COO), 159.74 (C4 CB), 157.11 (C3 Es), 145.37 (C1′ CB), 138.10 (C5 Es), 138.02 (–C=, C4 alkenyloxy) 132.71 (C3′,5′ CB), 132.51 (C10 Es), 131.55 (C1 CB), 128.52 (C2,6 CB), 127.22 (C2′,6′ CB), 126.44 (C1 Es), 119.28 (CN), 115.27 (C3,5 CB), 115.21 (C=, C5 alkenyloxy) 114.65 (C4 Es), 112.17 (C2 Es), 110.23 (C4′ CB), 82.83 (C17 Es), 67.70 (C–O, C6 alkanoate), 67.22 (C–O, C1 alkenyloxy) 49.92 (C14 Es), 43.94 (C13 Es), 43.15 (C9 Es), 38.73-21.93 (C6,7,8,11,12,15,16 Es, C2-3 alkenyloxy, C2-5 alkanoate), 12.31 (C18 Es).

3.1.19. *3-(5-Hexenyloxy)estra-1,3,5(10)-triene-17β-yl 6-(4′-cyanobiphenyl-4-yloxy)hexanoate (6Es6CB)*

Yield: 67%, $C_{43}H_{51}NO_4$ Ms(ESI): *m/z*: 663.8 (100%$(M+NH_4)^+$, calc.: 663.4), 646.8 (21%$(M+H)^+$, calc.: 646.4). ^{1}H NMR (300 MHz, $CDCl_3$) δ (ppm): 0.84 (s, 3H, CH_3, C18 (Es)), 1.15–2.49 (m, 27H, CH_2 and CH, C7-16 (Es), C2-4 (alkenyloxy) and C2-5 (alkanoate)), 2.84 (m, 2H, CH_2, C6 (Es)), 3.95 (t, $^3J = 6.43$ Hz, 2H, $CH_2OAr_{(Es)}$), 4.02 (t, $^3J = 6.43$ Hz, 2H, $CH_2OAr_{(CB)}$), 5.00 (m, $^3J_{cis} = 10.22$ Hz, 1H, H(*E*)H(*Z*)C=), 5.07 (m, $^3J_{trans} = 17.10$ Hz, 1H, H(*E*)H(*Z*)C=), 5.86 (ddt, $^3J_{trans} = 17.04$ Hz, $^3J_{cis} = 10.11$ Hz, $^3J = 6.71$ Hz, 1H, –CH=), 6.63 (d, $^4J = 2.57$ Hz, 1H, ArH, C4 (Es)), 6.70 (dd, $^4J = 2.57$ Hz, $^3J = 8.46$ Hz, 1H, ArH, C2 (Es)), 7.00 (m, $^3J = 6.62$ Hz, 2H, ArH, C3+5 (CB)), 7.20 (d, $^3J = 8.46$ Hz, 1H, ArH, C1 (Es)), 7.54 (m, $^3J = 6.62$ Hz, 2H, ArH, C2+6 (CB)), 7.65 (m, $^3J = 6.62$ Hz, 2H, ArH, C2′+6′ (CB)), 7.70 (m, $^3J = 6.62$ Hz, 2H, ArH, C3′+5′ (CB)). ^{13}C NMR (90 MHz, $CDCl_3$) δ (ppm): 173.58 (COO), 159.72 (C4 CB), 157.11 (C3 Es), 145.40 (C1′ CB), 138.08 (C5 Es), 137.97 (–C=, C5 alkenyloxy) 132.71 (C3′,5′ CB), 132.45 (C10 Es), 131.58 (C1 CB), 128.51 (C2,6 CB), 127.22 (C2′,6′ CB), 126.43 (C1 Es), 119.32 (CN), 115.27 (C3,5 CB), 115.12 (C=, C6 alkenyloxy) 114.62 (C4 Es), 112.16 (C2 Es), 110.19 (C4′ CB), 82.81 (C17 Es), 67.65 (C–O, C6 alkanoate), 67.19 (C–O, C1 alkenyloxy) 49.94 (C14 Es), 43.94 (C13 Es), 43.14 (C9 Es), 38.73–21.92 (C6,7,8,11,12,15,16 Es, C2-4 alkenyloxy, C2-5 alkanoate), 12.29 (C18 Es).

3.1.20. *3-(4-Pentenyloxy)estra-1,3,5(10)-triene-17β-yl 10-(4′-cyanobiphenyl-4-yloxy)undecanoate (5Es11CB)*

Yield: 75%, $C_{47}H_{59}NO_4$ Ms(ESI): *m/z*: 719.7 (100%$(M+NH_4)^+$, calc.: 719.5), 703.0 (15%$(M+H)^+$, calc.: 703.0). ^{1}H NMR (300 MHz, $CDCl_3$) δ (ppm): 0.84 (s, 3H, CH_3, C18 (Es)), 1.15–2.49 (m, 35H, CH_2 and CH, C7-16 (Es), C2-3 (alkenyloxy) and C2-10 (alkanoate)), 2.84 (m, 2H, CH_2, C6 (Es)), 3.95 (t, $^3J = 6.43$ Hz, 2H, $CH_2OAr_{(Es)}$), 4.02 (t, $^3J = 6.43$ Hz, 2H, $CH_2OAr_{(CB)}$), 5.00 (m, $^3J_{cis} = 10.22$ Hz, 1H, H(*E*)H(*Z*)C=), 5.07 (m, $^3J_{trans} = 17.10$ Hz, 1H, H(*E*)H(*Z*)C=), 5.86 (ddt, $^3J_{trans} = 17.04$ Hz, $^3J_{cis} = 10.11$ Hz, $^3J = 6.71$ Hz, 1H, –CH=), 6.63 (d, $^4J = 2.57$ Hz, 1H, ArH, C4 (Es)), 6.70 (dd, $^4J = 2.57$ Hz, $^3J = 8.46$ Hz, 1H, ArH, C2 (Es)), 7.00 (m, $^3J = 6.62$ Hz, 2H, ArH, C3+5 (CB)), 7.20 (d, $^3J = 8.46$ Hz, 1H, ArH, C1 (Es)), 7.54 (m, $^3J = 6.62$ Hz, 2H, ArH, C2+6 (CB)), 7.65 (m, $^3J = 6.62$ Hz, 2H, ArH, C2′+6′ (CB)), 7.70 (m, $^3J = 6.62$ Hz, 2H, ArH, C3′+5′ (CB)). ^{13}C NMR (90 MHz, $CDCl_3$) δ (ppm): 174.12

(COO), 159.95 (C4 CB), 157.17 (C3 Es), 145.44 (C1′ CB), 138.10 (C5 Es), 138.01 (–C=, C4 alkenyloxy) 132.74 (C3′,5′ CB), 132.49 (C10 Es), 131.56 (C1 CB), 128.47 (C2,6 CB), 127.22 (C2′,6′ CB), 126.42 (C1 Es), 119.29 (CN), 115.23 (C3,5 CB), 114.63 (C=, C5 alkenyloxy) 114.63 (C4 Es), 112.18 (C2 Es), 110.17 (C4′ CB), 82.61 (C17 Es), 68.31 (C–O, C11 alkanoate), 67.21 (C–O, C1 alkenyloxy) 49.92 (C14 Es), 43.95 (C13 Es), 43.15 (C9 Es), 38.73–21.94 (C6,7,8,11,12,15,16 Es, C2-3 alkenyloxy, C2-10 alkanoate), 12.31 (C18 Es).

3.1.21. *3-(10-Undecenyloxy)estra-1,3,5(10)-triene-17β-yl 10-(4′-cyanobiphenyl-4-yloxy)undecanoate (11Es11CB)*

Yield: 74%, $C_{53}H_{71}NO_4$ Ms(ESI): *m/z*: 803.4 (100%$(M+NH_4)^+$, calc.: 803.6), 786.6 (10%$(M+H)^+$, calc.: 786.5). ^{1}H NMR (300 MHz, $CDCl_3$) δ (ppm): 0.84 (s, 3H, CH_3, C18 (Es)), 1.15–2.49 (m, 47H, CH_2 and CH, C7-16 (Es), C2-9 (alkenyloxy) and C2-10 (alkanoate)), 2.84 (m, 2H, CH_2, C6 (Es)), 3.92 (t, $^3J = 6.62$ Hz, 2H, $CH_2OAr_{(Es)}$), 4.02 (t, $^3J = 6.62$ Hz, 2H, $CH_2OAr_{(CB)}$), 4.71 (dd, $^3J = 8.82$ Hz, $^3J = 7.72$ Hz, 1H, CH, C17 (Es)), 4.94 (m, $^3J_{cis} = 10.15$ Hz, 1H, H(*E*)H(*Z*)C=), 5.01 (m, $^3J_{trans} = 17.19$ Hz, 1H, H(*E*)H(*Z*)C=), 5.83 (ddt, $^3J_{trans} = 16.97$ Hz, $^3J_{cis} = 10.23$ Hz, $^3J = 6.66$ Hz, 1H, –CH=), 6.63 (d, $^4J = 2.57$ Hz, 1H, ArH, C4 (Es)), 6.70 (dd, $^4J = 2.57$ Hz, $^3J = 8.46$ Hz, 1H, ArH, C2 (Es)), 7.00 (m, $^3J = 6.62$ Hz, 2H, ArH, C3+5 (CB)), 7.19 (d, $^3J = 8.46$ Hz, 1H, ArH, C1 (Es)), 7.54 (m, $^3J = 6.62$ Hz, 2H, ArH, C2+6 (CB)), 7.65 (m, $^3J = 6.62$ Hz, 2H, ArH, C2′+6′ (CB)), 7.70 (m, $^3J = 6.62$ Hz, 2H, ArH, C3′+5′ (CB). ^{13}C NMR (90 MHz, $CDCl_3$) δ (ppm): 174.12 (COO), 159.95 (C4 CB), 157.17 (C3 Es), 145.44 (C1′ CB), 139.39 (C5 Es), 137.98 (–C=, C10 alkenyloxy) 132.72 (C3′,5′ CB), 132.42 (C10 Es), 131.39 (C1 CB), 128.47 (C2,6 CB), 127.22 (C2′,6′ CB), 126.42 (C1 Es), 119.29 (CN), 115.23 (C3,5 CB), 114.60 (C=, C11 alkenyloxy) 114.28 (C4 Es), 112.17 (C2 Es), 110.17 (C4′ CB), 82.61 (C17 Es), 68.31 (C–O, C11 alkanoate), 68.03 (C–O, C1 alkenyloxy) 49.92 (C14 Es), 43.95 (C13 Es), 43.13 (C9 Es), 38.75–23.44 (C6,7,8,11,12,15,16 Es, C2-9 alkenyloxy, C2-10 alkanoate), 12.28 (C18 Es).

All products were purified until single spots on silica gel thin layer chromatograms were obtained (Merck 60, F254 preformed aluminium plates) and their structures were confirmed by ^{1}H/^{13}C NMR (Bruker NMR AC300) and electrospray mass spectrometry (Micromass Platform quadrupole mass analyser, capillary 3.50 kV, HV lens 0.5 kV, cone voltage 20 V, source temperature 110°C, electrospray eluent: 100% acetonitrile at 100 μl min^{-1}, nitrogen drying gas 300 l h^{-1}, nebulizing gas 20 l h^{-1}, 10 μl injections of 1–10 μg ml^{-1} solutions using an HP 1050 autosampler).

3.2. *Materials characterization*

The liquid crystalline phases were characterized by differential scanning calorimetry (DSC) and optical microscopy. The DSC thermograms were obtained on a Perkin-Elmer DSC-7 system, using sample sizes of 2 to 5 mg at a scanning rate of 5 K min^{-1}. An Olympus BH-2 polarizing microscope, equipped with a Linkam TMS 90 heating stage, was used to observe the phase transitions and to study the mesophase textures of the materials. For observation and electro-optic measurements, the samples were allowed to capillary fill 4 μm thick glass sample cells. The inside walls of the cells carried transparent ITO electrodes and rubbed polyimide alignment layers (for planar alignment). The Cano wedge technique [16], using PTFE-treated [17] wedge-shaped cells, was employed to measure the pitch lengths of the chiral nematic liquid crystals. The polarizing microscope, in conjunction with a series of coloured filters, was utilized to determine helical sense by observing the effect of the optical rotatory power of the chiral nematic material on the polarized light transmitted by the sample [18].

3.3. *Electro-optical measurements*

In order to make electro-optical measurements, the polarizing microscope was equipped with a photodiode as the light detector. The waveforms of the fields applied across the specimens were either triangle- or square-waves, usually in the frequency range 10 Hz–1 kHz. The photodiode output signal and the applied voltage were monitored using a digitizing oscilloscope and the applied fields were varied in amplitude from zero up to 15 V μm^{-1}.

Magnitudes of the critical fields required to cause texture changes were evaluated by monitoring the changes in the intensity of the light transmitted by the material held between parallel polarizers, as the amplitude of the voltage applied across the cell was varied.

The field-induced tilt angles of the macroscopic optic axis were evaluated by holding a sample with its helical axis aligned in a uniform direction lying in the plane of the cell (the uniformly-lying helix texture [3, 10]) between crossed polarizers and measuring the half-angle between the two extinction positions. Low frequency (30 to 80 Hz) alternating voltages with a square waveform were employed to ensure complete switching. The uniformly lying helix texture was obtained by applying a field slightly greater than the critical field required to form the focal-conic texture, while unidirectionally rubbing the cell. The rubbing action promotes alignment via a shearing action, forcing the helix to lie parallel to the cell walls and perpendicular to the rubbing direction.

Response times were defined as the time elapsed between a change in polarity of the applied field and

the responding photodiode signal changing from 0 to 90% of its peak-to-peak amplitude. In making these measurements, the sample was aligned such that the helical axis was at 22.5° to the transmission axis of one of the microscope polarizers.

3.4. *UV-vis spectroscopy*

Maximum reflected wavelengths of planar-aligned chiral nematic liquid crystals were evaluated as a function of temperature using an HP 8453 UV-visible spectrophotometer and a Mettler FP 82 heating stage with an FP 80 controller. The spectrum transmitted by the sample held normal to the light beam was measured. Reference measurements were made with the sample in the isotropic phase. The maximum reflected wavelength was measured at the midpoint in the absorbance peak produced in the transmitted light by back reflection due to the helical pitch.

3.5. *Molecular modelling*

Molecular modelling was performed with the desktop modelling software Chem3D from Cambridge Scientific. A trial molecular structure with alkyl chains in the all-*trans*-conformation was built and energy-minimized using the MM2 force field. The dihedral angles of the ester and the two ether linkages were subsequently adjusted and the conformational energy profile of each torsional angle was calculated. The local energy minima were identified and individually optimized using MOPAC/PM3.

4. Results and discussion

4.1. *Phase classification*

Phase transition temperatures, enthalpies and entropies are given in table 1. The bimesogens with odd numbers n of carbon atoms in the second spacer exhibit chiral nematic mesophases, identified by their planar Grandjean textures and characteristic oily streak defects. An even number of carbon atoms in the second spacer destabilizes the mesophase. 5Es6CB displays only a monotropic chiral nematic phase, while 6Es6CB is not liquid crystalline. Inspection of the 3-dimensional structures of 5Es5CB and 5Es6CB, as derived from MOPAC/PM3 calculations, shows that only for an odd number n of flexible units in the second spacer are both mesogenic moieties aligned parallel, as required for good ordering in the mesophase (figure 4) [19]. This is also reflected in the entropy change at the clearing temperature, which is less than half as much for 5Es6CB compared with the other compounds with odd-numbered second spacers.

Included in table 1 are the helical pitch lengths of the chiral nematic liquid crystals, measured using the Cano wedge technique. The present materials have left-handed helicity. Figure 5 illustrates the variation in maximum reflected wavelength as a function of reduced

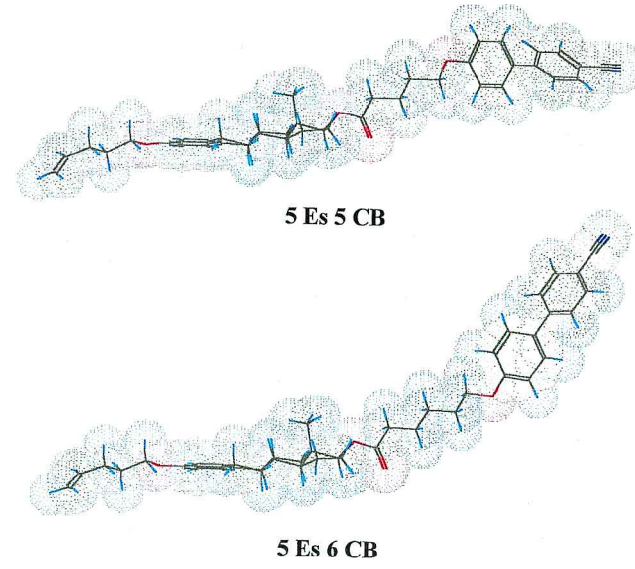

Figure 4. 3D structures of compounds 5Es5CB and 5Es6CB as obtained by molecular modelling.

Table 1. Phase transition temperatures, enthalpies, and entropies as obtained from DSC thermograms and helical pitches measured by the Cano wedge technique.

Compound *m*Es*n*CB	Transition temperature[a]/°C	Pitch length /nm (T_r/°C)[b]	$\Delta H_{N^*\text{-}I}$[c] /kJ mol^{-1}	$\Delta S_{N^*\text{-}I}$[c] /J K^{-1} mol^{-1}
5Es5CB	Cr 91 N* 105 I	320 (– 4)	– 2.5	– 6.5
5Es6CB	Cr 105 (N* 83)[c] I	< 200[d]	– 1.1	– 3.1
6Es5CB	Cr 61 N* 96 I	312 (– 5)	– 2.8	– 7.7
6Es6CB	Cr 65 I	—	—	—
11Es5CB	Cr 68 N* 95 I	595 (– 5)	– 2.7	– 7.5
5Es11CB	Cr 71 N* 87 I	210 (– 5)	– 2.8	– 7.7
11Es11CB	Cr 42 N* 82 I	286 (– 10)	– 3.9	– 10.9

[a] Taken from DSC thermograms on second heating.
[b] Reduced temperature, $T_r = T - T_{clear}$.
[c] Taken from DSC thermograms on second cooling.
[d] Pitch length smaller than the visible range.

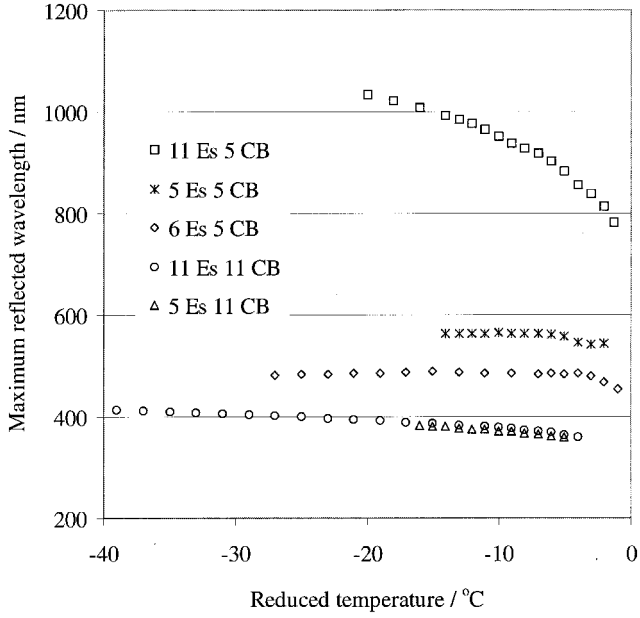

Figure 5. Maximum reflected wavelengths as a function of temperature for the compounds showing chiral nematic mesophases.

temperature: the selectivity reflected wavelengths vary little with temperature for most of the materials.

The monotropic material 5Es6CB in its chiral nematic phase does not reflect light in the visible spectrum, indicating that it has an extremely short pitch. Indeed, in a contact preparation with 11Es5CB, selective reflection across the visible spectrum is observed over a narrow concentration gradient. Apparently, non-parallel alignment of the mesogenic units in 5Es6CB causes a significant increase in the helical twisting power of this chiral nematic mesophase over that of 5Es5CB.

Clearly, the individual alkyl spacer lengths m and n have a strong influence on the helical pitch:

(1) Increasing the number n of carbon atoms in the second spacer from 5 to 11 leads to a drastic decrease in pitch length for constant m.
(2) Increasing the number m of carbon atoms in the terminal chain from 5 to 11 leads to an increase in pitch length of varying extent for constant n.

In order to explain this behaviour one has to take into account the different properties of the two component mesogenic units in these compounds. The estradiol units impose a twist on the phase due to chiral coupling. This effect is counteracted by the dipolar interactions between the cyanobiphenyl groups of adjacent molecules, which favour antiparallel alignment [20]. Therefore, the decoupling of these two moieties by a long second spacer should allow for a higher twist in the mesophase and thus a shorter pitch length, as observed in our materials. Accordingly, the non-parallel alignment of the two mesogenic units in 5Es6CB would not allow for strongly stacking dipole–dipole interactions of the cyanobiphenyl groups in the mesophase. Therefore, the twisting angle in this material should be increased, resulting in the observed shorter pitch length compared with 5Es5CB, with its parallel-oriented mesogenic units.

It has been suggested for chiral nematic twin and triplet mesogens, that the dependence of the pitch on the spacer length is a result of different degrees of order in the mesophase [19, 21, 22]. For compounds with parallel-oriented mesogenic units, the fraction of bent rotamers increases with increasing spacer length. It has been argued that this leads to a less ordered chiral nematic phase and therefore to higher twisting angles. While this explanation could account for the observed trend in the pitch lengths of our materials, it is not in agreement with the observed transition entropies, which generally increase with decreasing pitch. Similar results for the relationship between pitch and $\Delta S_{N^*\text{-}I}$ in chiral nematic bi- and tri-mesogenic compounds have been reported in literature [21, 22].

The increase of the pitch with increasing length of a terminal chain has been reported previously for liquid crystal materials possessing right handed helices [23, 24]. In the case of estradiol as the steroidal unit, one can understand this in terms of the terminal chain (increasing m) diluting the chiral nematic mesophase by increasing the number of non-chiral interactions.

4.2. *Critical fields*

The present materials have positive dielectric anisotropies: at high field amplitudes ($\sim 10\ \mathrm{V\ \mu m^{-1}}$) the molecules tend to align along the applied field direction. The sequence of textures observed in these chiral nematic materials on increasing or decreasing the field is shown schematically in figure 6. On applying an increasing field across a Grandjean texture, see figure 7(*a*), parallel to the helical axis, the transition to the grid and stripe texture [25] may be observed as the helices begin to tilt under the effect of the field. As the helices tilt still further with respect to the applied field, the focal-conic texture forms. Figure 7(*b*) shows focal-conic regions forming in the grid texture of 11Es5CB. Increasing the field amplitude further causes the helix to unwind and at some critical field the homeotropic nematic texture forms as the pitch becomes infinite.

The critical fields at reduced temperatures of about -1°C are given in table 2. The relatively low field strengths required for complete unwinding of the helix attest to the high dielectric anisotropies conferred on these materials by the highly polar cyanobiphenyl group. Regarding the transitions between the focal-conic texture and the homeotropic nematic texture on increasing and

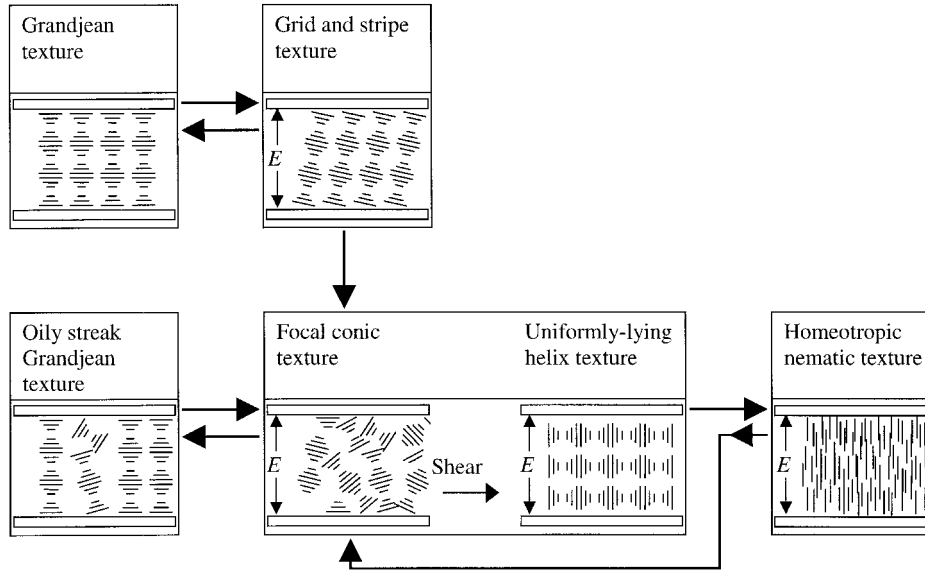

Figure 6. Sequence of textures observed on increasing (→) and decreasing (←) the amplitude of the field applied across a chiral nematic material with positive dielectric anisotropy.

Table 2. Critical fields measured on increasing and decreasing the amplitude of the voltage applied across the samples. Measurements were obtained at reduced temperatures of about – 1°C. The critical field estimates for the monotropic material 5Es6CB are quoted to fewer significant figures because these measurements were obtained very quickly, before crystallization could occur.

	Critical field/V μm^{-1}			
Compound *m*Es*n*CB	Grandjean →focal conic	Oily streak Grandjean →focal conic	Focal conic→ homeotropic nematic	Homeotropic nematic →focal conic
5Es5CB	1.65	0.94	5.65	5.06
5Es6CB	7	—	19	19
6Es5CB	1.98	1.30	7.36	6.97
11Es5CB	1.59	0.85	4.32	3.85
5Es11CB	2.43	1.35	11.05	10.24
11Es11CB	3.61	1.33	14.50	14.45

decreasing the field strength, some hysteretic behaviour is observed. This effect has been described previously [26, 27].

The spacer substitution on the estradiol unit has a profound influence on the electro-optic properties of the material. Critical fields increase as the length of the second spacer increases, a trend that is particularly obvious when comparing the transitions between the focal-conic and the homeotropic nematic textures. The critical field for such a transition varies as P_0^{-1} [28] and thus the general trend is related to the decrease in pitch length as the second spacer increases in length. 5Es6CB apparently has a very short pitch length, leading to very high critical fields in comparison with the other materials. Comparing 6Es5CB, 5Es5CB and 11Es5CB, the critical field strengths decrease with increasing pitch lengths. In the case of 11Es11CB and 5Es11CB the trend is broken, as 11Es11CB has a slightly longer pitch than 5Es11CB but exhibits higher critical fields. However, the different alkyl chain lengths in 5Es11CB might hinder effective packing in the chiral nematic phase, reducing the field strength necessary to cause a transition. The low transition entropy of 5Es11CB compared with 11Es11CB supports this supposition.

4.3. *Flexoelectro-optic behaviour*

The flexoelectro-optic behaviour of the materials 5Es5CB, 11Es5CB, 5Es11CB, and 11Es11CB was investigated. The effect of temperature on the induced tilt angle of the optic axis was observed. Figure 8 (*a*) shows data obtained for 5Es5CB. The tilt angle of the optic axis increases with temperature, a trend not predicted by the foregoing theory, as the material's non-negligible, temperature-dependent dielectric anisotropy couples with the relatively large applied field. This increase in tilt angle with temperature cannot, however, be ascribed

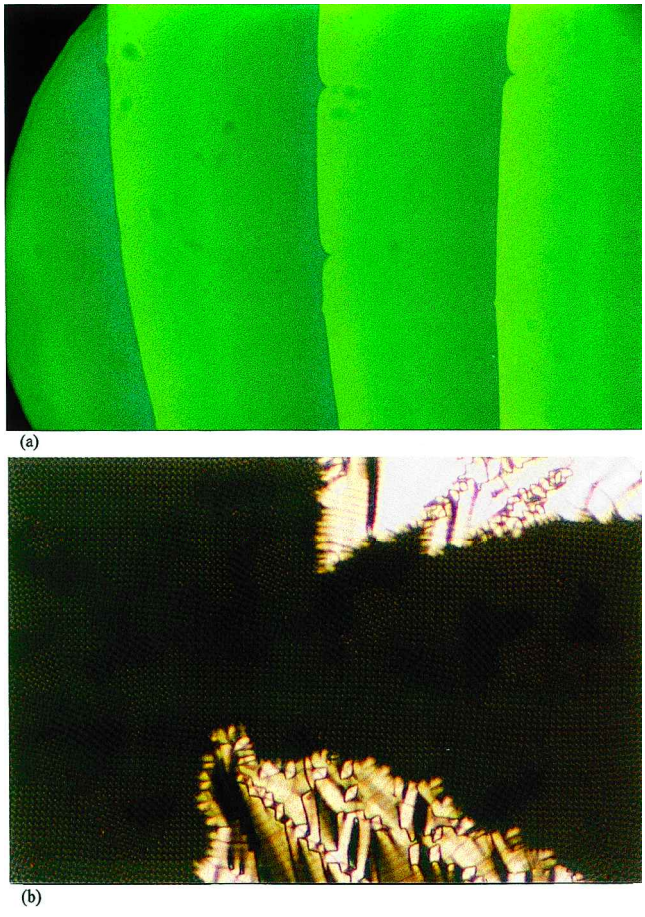

Figure 7. Photomicrographs showing (*a*) the Grandjean texture, with disclinations, of 5Es5CB at 104°C, magnification 28×, and (*b*) the grid texture of 5Es11CB with encroaching focal conic regions, at 94°C, with an applied field amplitude of 4.1 V μm^{-1}, magnification 134×.

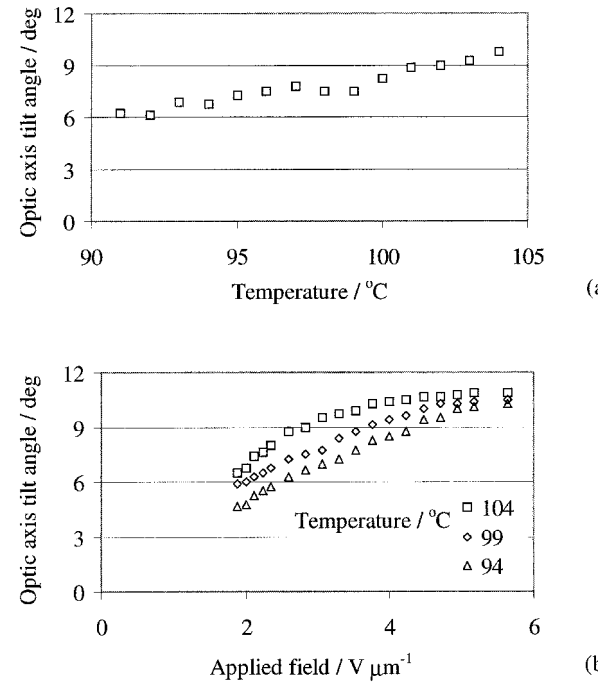

Figure 8. Field-induced tilt angle of optic axis as a function of temperature (*a*), at a constant field of 2.5 V μm^{-1}, and as a function of applied field (*b*), for the material 5Es5CB.

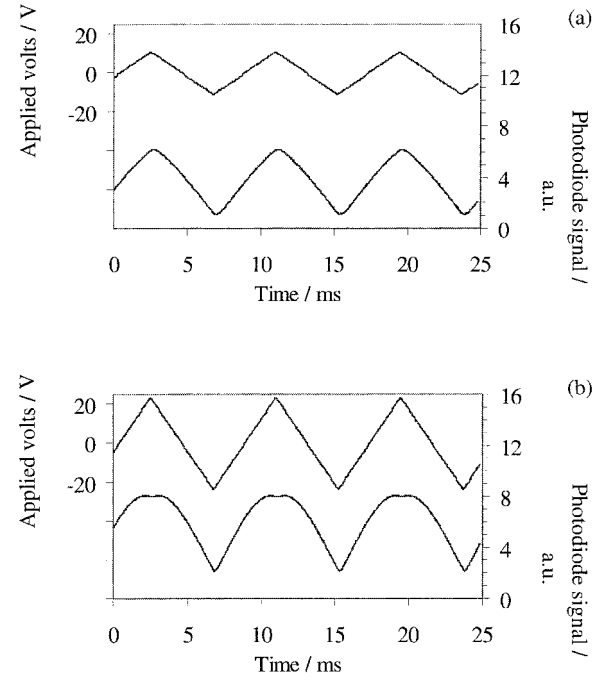

Figure 9. Linear flexoelectro-optic response (*a*) and deformation due to high fields (*b*). In (*a*) $T = 75°C$, $E_{max} = 2.9$ V μm^{-1}, $f = 59$ Hz; in (*b*) $T = 88°C$, $E_{max} = 6.3$ V μm^{-1}, $f = 59$ Hz. The material is 5Es11CB.

to the temperature-dependence of the helical pitch, since in all of the present materials there is a decrease in pitch as the temperature increases. [Equation (3) indicates that a decrease in pitch length would cause the tilt angle to decrease.]

The effect of an increasing field on the induced tilt angle was also examined. Figure 8 (*b*) illustrates that for 5Es5CB the relationship between the tilt angle and the amplitude of the electric field is non-linear, attesting to helix-unwinding, even under the influence of moderate electric fields ($E \approx 2$ V μm^{-1}). At low fields, as predicted by equation (3), the flexoelectro-optic response is linear in E, see figure 9 (*a*). Here we show the response to a triangular wave. At higher fields and temperatures the electro-optic effect is distorted by dielectric coupling as shown in figure 9 (*b*). The response to a bipolar square wave is shown in figure 10 (*a*) where the switching time is typically, for 5Es11CB, of the order of 280 μs. The field free relaxation, for a monopolar pulse of the same

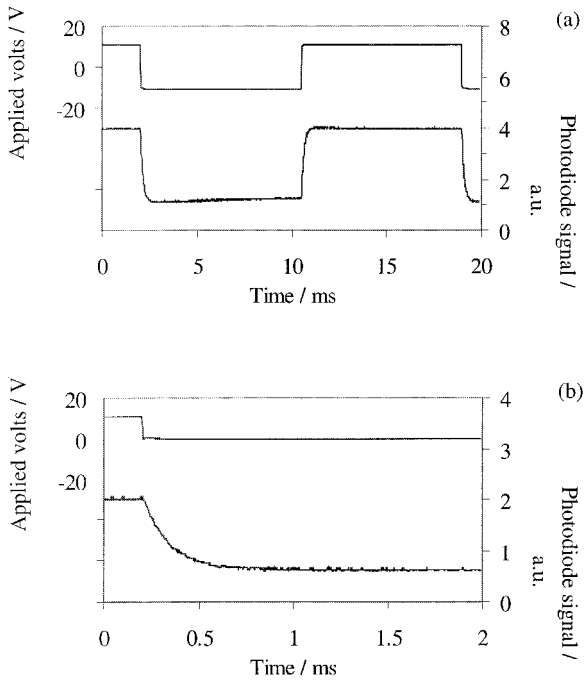

Figure 10. Flexoelectro-optic response to (*a*) a bipolar square wave and (*b*) a monopolar pulse. In both cases $E = 2.9\ \mathrm{V\ \mu m^{-1}}$ and $T = 88°\mathrm{C}$; the material is 5Es11CB.

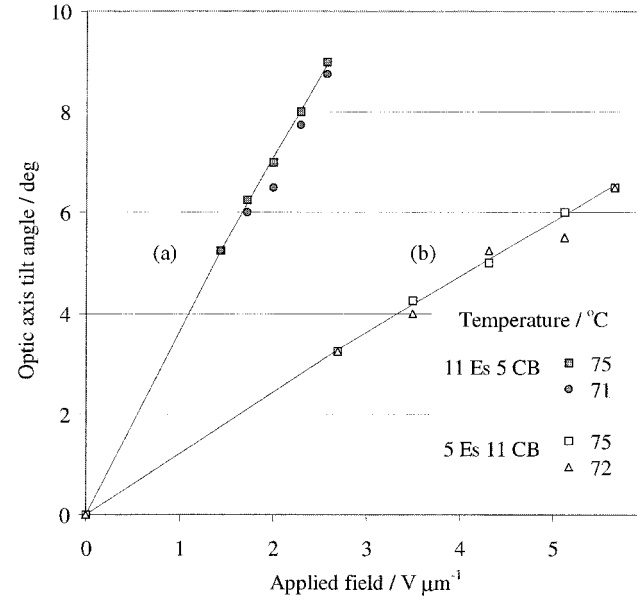

Figure 11. Optic axis tilt angle versus applied field for (*a*) 11Es5CB and (*b*) 5Es11CB.

Table 3. Flexoelectric coefficients of 5Es5CB and 11Es5CB.

Compound	$e/k\kappa$/m V^{-1}	Effective flexoelectric coefficient, e/C m^{-1}
11Es5CB	5.74×10^{-8}	-5.2×10^{-12}
5Es11CB	1.93×10^{-8}	-5.3×10^{-12}

amplitude is shown in figure 10(*b*). It is noteworthy that this decay time is fast for a (chiral) nematic material, i.e. 280 μs, and in this case is identical in both figures 10(*a*) and (*b*).

However, in low fields and over short temperature ranges, two of the materials in this series, 11Es5CB and 5Es11CB, do show a temperature-independent response, with tan ϕ proportional to the amplitude of the applied field, as shown in figure 11. The lines shown are linear regressions fitted to the 75°C data sets using equation (3).

The undisturbed pitch length of 5Es11CB at 75°C is 230 nm, measured using the Cano wedge technique. A direct measurement of the pitch of 11Es5CB was not possible at 75°C because the contrast was low; the selectively-reflected wavelength at this temperature is 1033 nm. Using data contained in table 1 and figure 6, we may apply the expression $\lambda_{refl} = nP_0$ to estimate that at a reduced temperature of $-5°\mathrm{C}$ the mean refractive index, n, of this material is 1.48. Making the assumption that n varies little with temperature, we estimate that the pitch length at 75°C is 700 nm. A reasonable value for the average elastic constant κ ($\kappa \approx 10^{-11}$ N [29]) was assumed. The results are shown in table 3. To the best of our knowledge, the values thus obtained for 5Es11CB [$e(\kappa^{-1}) = -0.53\ \mathrm{C\ N^{-1}\ m^{-1}}$] and 11Es5CB [$e(\kappa^{-1}) = -0.52\ \mathrm{C\ N^{-1}\ m^{-1}}$] are the highest published to date by almost an order of magnitude; previous work [2, 3, 14] has concerned materials with $0.03\ \mathrm{C\ N^{-1}\ m^{-1}} \leqslant e(\kappa^{-1}) \leqslant 0.12\ \mathrm{C\ N^{-1}\ m^{-1}}$.

The flexoelectro-optic response of the present materials is demonstrably very strong, with the optic axes tilting by up to 10° for applied fields of only 3–10 V μm^{-1}, compared with previous work [2, 3, 14, 30] where similar tilt angles, up to 10°, were observed for fields of 23–40 V μm^{-1}.

The characteristic response times (0–90% optical change) of our materials are shown in figure 12. The response times decrease with increasing temperature and, to a lesser degree, with increasing field amplitude. This is in agreement with the observations recorded in previous work [2, 31] although, according to equation (4), the response time should not depend on the field amplitude, since increasing the field increases the angular response speed, but also increases the saturation angle by the same proportion [14]. However, surface anchoring conditions have been shown to affect the dynamic properties of the electro-optic effect [31], thereby introducing a weak field dependence. There are several other significant characteristics of the flexoelectro-optic switching of the chiral nematic materials. Firstly, unlike the classical twisted nematic (TN) effect, there is no time

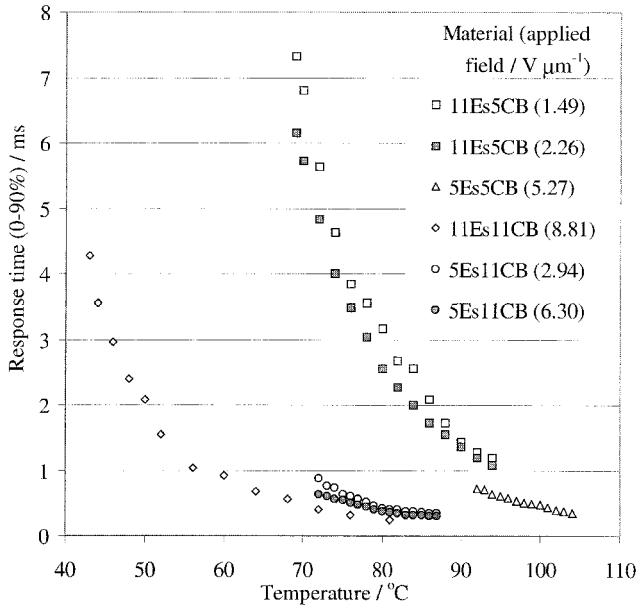

Figure 12. Response times as a function of temperature.

delay between application of the field and manifestation of the electro-optic effect, c.f. figure 10. Secondly, the effect is linear rather than quadratic in E. These features are important for driving waveforms in modulators or multiplexed devices. Thirdly, the response times, quoted for 0 to 90% optical change, are of at least an order of magnitude faster than those recorded for the TN effect driven under the same field and reduced temperature conditions. For example, at $T_{NI} - T \simeq 20°C$ and $E \approx 5\ V\ \mu m^{-1}$, the flexoelectro-optic response time is less than 1 millisecond. The field free decay time, driven by the helix returning to its quiescent state, is equally fast or faster.

5. Conclusions

A new series of bimesogenic chiral nematic materials based on β-estradiol and 4-cyanobiphenyl was synthesized. These materials, although possessing a high dielectric anisotropy, open up for the first time the possibility of using the flexoelectro-optic response of a pure chiral nematic material for display applications:

(1) The materials have short and almost temperature-independent pitch lengths, which may be selected by using appropriate alkyl chain lengths. A longer spacer chain length between the two mesogenic units and/or a short terminal alkyl chain favour shorter helix pitches.

(2) The flexoelectric coefficients are the largest observed thus far in any chiral nematic material and the optical tilt is linear in field if unequal spacer lengths are employed. The materials show high tilt angles per unit monopolar applied field. For bipolar square waves the optical tilt angle is doubled on field reversal. Thus the switching angles for an a.c. square wave are twice those reported in figure 11. For a crossed polarizer/analyser pair, the maximum optical tilt required is thus 22.5° for maximum light transmission. Good contrast can still be achieved for lower angles since the transmission curve varies as a $\sin^2$ function.

(3) The materials have millisecond, or faster, response times at moderately low field strengths, i.e. a few $V\ \mu m^{-1}$ and these response times only show a weak field dependence. Thus typical cells of 2–4 μm thickness may readily be switched by CMOS or TTL voltage levels.

In summary these bimesogenic asymmetric liquid crystal materials show interesting flexoelectro-optic properties that indicate their potential for applications to optical modulators and devices. In order to reduce the operating temperatures to room temperature and further improve response times, we are currently modifying the structure of the achiral mesogen and the flexible chains as well as using the current mesogens in mixtures with low viscosity nematogens. This work [32] will be reported at a later date. We have also synthesized similar bimesogens attached via a hydrosilylation reaction to linear and cyclic organosiloxane moieties. The latter materials allow us to alter the asymmetric molecular shape, and thereby influence the flexoelectro-optic properties, as well as induce glass transitions that allow optical storage of the switched states. It is clear that studies on such properties are at an early stage, but we anticipate that further molecular engineering should lead to a rapid optimization of the flexoelectro-optic effect in chiral nematic materials.

B.M. and P.L. acknowledge studentship support from the EPSRC and Merck (UK), respectively, and all three authors thank Prof. Lachezar Komitov of the Chalmers Liquid Crystal Group for invaluable discussions.

References

[1] Rudquist, P., Carlsson, T., Komitov, L., and Lagerwall, S. T., 1997. *Liq. Cryst.*, **22,** 445.

[2] Rudquist, P., Buivydas, M., Komitov, L., and Lagerwall, S. T., 1994, *J. appl. Phys.*, **76,** 7778.

[3] Patel, J. S., and Meyer, R. B., 1987, *Phys. Rev. Lett.*, **58,** 1538.

[4] Hermann, D. S., Rudquist, P., Ichimura, K., Kudo, K., Komitov, L., and Lagerwall, S. T., 1997, *Phys. Rev. E*, **55,** 2857.

[5] Hermann, D. S., Komitov, L., Lagerwall, S. T., Heppke, G., and Rauch, S., 1998, Poster 57. Presented at the 27th Freiburg Liquid Crystal Workshop. 25–27 March 1998, Freiburg, Germany; Hermann, D. S., Komitov, L., Lagerwall, S. T., Heppke, G., and

RAUCH, S., 1998, *Flexoelectric Polarization Changes Induced by Bent-Shape Molecules Dissolved in a Nematic Liquid Crystal*. Presented at the 17th International Liquid Crystal Conference. 19–24 July, 1998, Strasbourg, France.

[6] PETROV, A. G., IONESCU, A. TH., VERSACE, C., and SCARAMUZZA, N., 1995, *Liq. Cryst*., **19,** 169.

[7] MEYER, R. B., 1969, *Phys. Rev. Lett*., **22,** 918.

[8] RUDQUIST, P., and LAGERWALL, S. T., 1997, *Liq. Cryst*., **23,** 503.

[9] MÜLLER, W. U., and STEGEMEYER, H., 1973. *Ber. Buns.-Ges. Phys. Chem*., **77,** 20.

[10] KOMITOV, L., LAGERWALL, S. T., STEBLER, B., and STRIGAZZI, A., 1994, *J. appl. Phys*., **76,** 3762.

[11] VERTOGEN, G., and DE JEU, W. H., 1988, *Thermotropic Liquid Crystals, Fundamentals*, Springer series in Chemical Physics 45 (Berlin: Springer-Verlag).

[12] OSIPOV, M. A., 1983, *Sov. Phys. JETP*, **58,** 1167.

[13] OSIPOV, M. A., 1984, *J. Physique Lett*., **45,** L-823.

[14] PATEL, J. S., and LEE, S.-D., 1989, *J. appl. Phys*., **66,** 1879.

[15] DE GENNES, P. G., and PROST, J., 1993, *The Physics of Liquid Crystals*, 2nd Edn (Oxford: Oxford Science Publications, Clarendon Press).

[16] CANO, R. R., 1968, *Bull. Soc. Miner. Cryst*., **91,** 20.

[17] MEYER, S., 1995, PhD thesis, Université Louis Pasteur, Strasbourg.

[18] COLES, H. J., 1998, in *Handbook of Liquid Crystals*, Vol. 2A, edited by D. Demus, J. Goodby, G. W. Gray, H.-W. Spiess, and V. Vill (Weinheim, New York, Chichester, Brisbane, Singapore, Toronto: Wiley-VCH), Chap. 2, pp. 339–341.

[19] MARCELIS, A. T. M., KOUDIJS, A., and SUDHÖLTER, E. W. C., 1996, *Liq. Cryst*., **21,** 87.

[20] LISETSKI, L. N., and TOLMACHEV, A. V., 1989, *Liq. Cryst*., **5,** 877.

[21] MARCELIS, A. T. M., KOUDIJS, A., and SUDHÖLTER, E. W. C., 1995, *Liq. Cryst*., **18,** 843.

[22] MARCELIS, A. T. M., KOUDIJS, A., and SUDHÖLTER, E. W. C., 1995, *Liq. Cryst*., **18,** 851.

[23] LEDER, L. B., 1971, *J. chem. Phys*., **54,** 4671.

[24] LEDLER, L. B., 1973, *J. chem. Phys*., **58,** 1118.

[25] VERTOGEN, G., and VAN GROESEN, E. W. C., 1982, *J. chem. Phys*., **76,** 2043.

[26] LIN-HENDEL, C. G., 1982, *J. appl. Phys*., **53,** 916.

[27] VAN SPRANG, H. A., and VAN DE VENNE, J. L. M., 1985, *J. appl. Phys*., **57,** 175.

[28] DE GENNES, P. G., 1968, *Solid State Commun*., **6,** 163.

[29] DE JEU, W. H., 1981, *Mol. Cryst. liq. Cryst*., **63,** 83.

[30] KOMITOV, L., LAGERWALL, S. T., SCHEROWSKY, G., and STEBLER, B., 1991, *Linear Electro-optic Response in the N* phase with Fingerprint Texture*. Presented at the European Conference on Liquid Crystals. 10–16 March 1991, Courmayeur, Valle d'Aosta, Italy.

[31] LEE, S.-D., PATEL, J. S., and MEYER, R. B., 1991, *Mol. Cryst. liq. Cryst*., **209,** 79.

[32] COLES, H. J., MUSGRAVE, B., and LEHMANN, P., 1998, *Mesogenic estradiols*, E.U. Patent Application No. EP 98 112 610.5 (filed July 1998).